

## Catalytic Hydrogenation of Crotonaldehyde in Trickle-bed Reactor

C. Uraz\*, F. Sami Atalay\*\*, and S. Atalay\*\*\*

Ege University, Faculty of Engineering, Department of Chemical Engineering,  
35100 Bornova-Izmir / TURKEY, Fax: 90(232)388 76 00

\*e-mail: uraz@eng.ege.edu.tr; \*\*e-mail: fsatalay@eng.ege.edu.tr;

\*\*\*e-mail: satalay@eng.ege.edu.tr

Original scientific paper

Received: March 17, 2003

Accepted: May 24, 2004

The liquid-phase hydrogenation of crotonaldehyde to *n*-butyraldehyde, was investigated. A palladium based commercial catalyst ( $w = 0.05$  % Pd on  $\text{Al}_2\text{O}_3$ ) was used in a laboratory scale trickle-bed reactor. The influence of temperature on the reaction, crotonaldehyde and hydrogen flow rates satisfying trickle flow conditions, and the appropriate space velocity LHSV and space time ranges, were searched. The operating conditions were proposed as the temperature range of 30 – 50 °C, the LHSV space velocity range of 2 – 7  $\text{h}^{-1}$ , and the space time ( $m_w/F_{\text{CAO}}$ ) range of 250 – 4108  $\text{g min mol}^{-1}$ , at constant hydrogen/crotonaldehyde molar ratio as 2:1, at atmospheric pressure. Kinetic experiments were performed to calculate the reaction rates and then to explore the rate expression in trickle-bed reactor. The data between space time and conversion were evaluated at the different studied temperatures and the relation between these parameters was derived by regression. The reaction rates were calculated by differentiation of the derived equations. The reaction rate expression was derived by using “Power Law” model. Kinetic parameters were calculated by taking into consideration external and internal mass transfer resistances.

*Key words:*

Liquid-phase hydrogenation, crotonaldehyde, *n*-butyraldehyde, trickle-bed reactor

### Introduction

Catalytic hydrogenation of crotonaldehyde is an industrially important reaction since the products (*n*-butanol and *n*-butyraldehyde) are very valuable chemical intermediates.

*n*-Butanol and *n*-butyraldehyde are produced by gas- or liquid-phase hydrogenation of crotonaldehyde, by complete hydrogenation or by partial hydrogenation of crotonaldehyde, obtained by the acetaldehyde route or by the oxo route.<sup>1,2,3</sup>

Most of the published information on the hydrogenation of crotonaldehyde relates to vapour phase reaction mechanisms. But only *Sedriks* and *Kenney* evaluated, both, vapour and liquid phase rates of hydrogenation of crotonaldehyde in a trickle-bed reactor and, from these rates, obtained the wetting factor of the catalyst bed. They also used a stirred basket reactor. They investigated the reaction over both pelleted and powdered catalyst having a composition of  $w = 0.5$  % Pd on alumina. They especially investigated the wetting of the catalyst bed; for this purpose two methods of packing were employed. In the first method, the cylindrical pellets were simply dumped on top of inert packing. The second method of packing consisted of interspersing catalyst pellets with small and low porosity alumina granules of irregular shape. By evaluating the experiments carried out at constant hydro-

gen inlet flow rate and pressure they derived overall reaction rate.<sup>4</sup> Other similar reactions are also investigated using trickle-bed reactor. Hydrogenation of  $\alpha$ -methyl styrene is studied by *Herskowitz* et al.<sup>5</sup> *Sharma* et al. investigated the benzene hydrogenation in a trickle-bed reactor.<sup>6</sup> Hydrogenation of 3-hydroxypropanal in trickle bed is studied by *Zhu* et al.<sup>7</sup>

The term trickle-bed is used to mean a reactor in which a liquid phase and a gas phase flow cocurrently downward through a fixed bed of catalyst particles while reaction takes place. Such reactors are widely used, particularly when one reactant is very volatile and another is normally a liquid, as in processes involving hydrogen (hydrogenation and desulfurization of oils) or oxygen (oxidation of liquid-phase reactants). Interphase mass transfer and wetting efficiency, as well as intraparticle diffusion and intrinsic kinetics, can affect the performance of such systems.<sup>4, 8, 9, 10</sup>

Different types of catalysts are used for the gas and liquid-phase hydrogenation of crotonaldehyde. For example an interesting study on the vapour-phase hydrogenation of crotonaldehyde over several supported Pt catalysts and on Pt powder is reported using different supports, precursors and pretreatments.<sup>11, 12</sup> The commonly used commercial hydrogenation catalysts are copper-chromite; cobalt

compounds; nickel compounds which may contain small amounts of chromium or other promoters; and mixtures of copper and nickel and/or chromium.<sup>13</sup>

Group VIII metals (Fe, Co, Ni, Ru, Rh, Pd, Os, Ir, Pt) are found to present good behavior as hydrogenation catalysts when supported on highly porous materials such as alumina. The catalysts consist mainly of one or more metallic phases—usually nickel, palladium or platinum and less frequently ruthenium, rhodium, cobalt or even iron, supported on highly porous materials, such as metallic oxides or activated charcoal.<sup>14,15</sup>

Selective hydrogenation of  $\alpha, \beta$ -unsaturated aldehydes is an interesting model reaction, as these molecules contain both C=O and C=C bonds; moreover, the latter are conjugated. Selective reduction of the C=O bond leaving the C=C bond intact is difficult. In the line of extensive research on strong metal-support interactions, the suitability of reducible oxides as supports was also tested in crotonaldehyde hydrogenation.<sup>16,17</sup>

The purpose of this study is to investigate the effect of the reaction parameters on the liquid-phase hydrogenation of crotonaldehyde in a laboratory scale trickle-bed reactor and to establish a model equation for the reaction rate fitting the experimental data.

## Experimental section

### Catalyst

The experiments were carried out on a palladium based commercial catalyst which has a pellet diameter of 3 mm (spherical). It was supplied from Süd Chemie company. The catalyst with a commercial name of Gridler (G-58B) has a composition of  $w = 0.05\%$  Pd on  $\text{Al}_2\text{O}_3$ . Its specifications are as follows: surface area  $s = 160 - 220 \text{ m}^2 \text{ g}^{-1}$ , bulk density  $\rho_b = 0.65 \text{ g cm}^{-3}$ . The catalyst was delivered in palladium oxide form. Before start-up, it was activated by reducing in hydrogen stream at atmospheric pressure and at a temperature of  $100^\circ\text{C}$ . The reduction lasted for 8 h at a flow rate of hydrogen of  $200 \text{ ml ml}_{\text{catalyst}}^{-1} \text{ h}^{-1}$ .<sup>18</sup>

### Materials

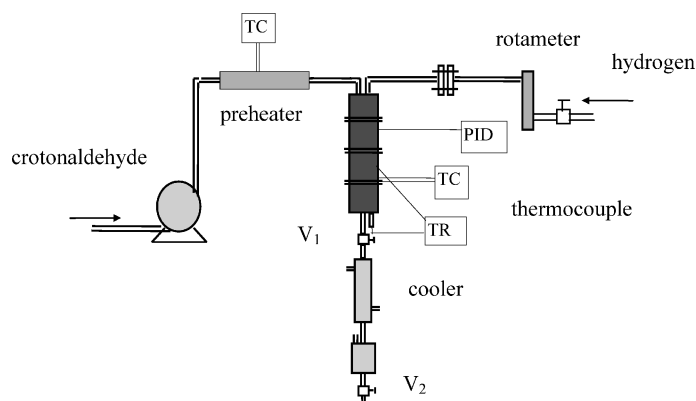
Crotonaldehyde produced by the company of Riedel de Haen was used as the liquid reactant. It was filled into a graduated glass cylinder and fed to the reactor using a variable speed peristaltic pump. A special plastic tube called PharMed, 0.8 mm diameter, was used to carry the liquid.

Hydrogen gas was supplied to the system using a  $8 \text{ m}^3$  of gas cylinder and its flow rate was adjusted

by the valve on a calibrated rotameter. The measured hydrogen gas was transported to the reactor passing through a stainless steel pipe.

### Apparatus

The experimental set-up (Fig.1) mainly consists of a preheater, a reactor and a cooler. All parts of the experimental set-up were made of stainless steel (SS 316).



PID : Proportional Integral Differential Controller

V : Valve

TC : Temperature Control

TR : Temperature Recorder

Fig. 1 – Experimental Set-Up

The trickle-bed reactor contains four parts: liquid distributor, primary inert part, catalyst bed, and secondary inert part.

The liquid distributor is shown in Figure 2. Eleven capillary tubes having an inner diameter of 0.9 mm and 15 mm length, are used to distribute the liquid and a plate having a lot of holes with 0.5 mm diameter is used to distribute the gas stream. The liquid distribution is one of the most important factors in the design and operation of trickle-bed reactors. It is usually admitted in the literature that, for all hydrodynamic regimes, the radial distribution of liquid flow can be considered as uniform over the cross-sectional area of the reactor, when the value of the ratio  $D_R/d_p$  is between some critical value. This critical value varies from 12 to 20 by several authors.<sup>19</sup> In this study, it is  $D_R/d_p = 42/3 = 14$ , so uniform liquid distribution might be obtained.

The catalyst bed is located between the inert packing parts. The reactor is heated electrically using Ni-Cr resistance wires, and its temperature is controlled from the outer surface by a PID temperature controller. The temperature of the reactor is recorded at the different bed positions by moving the thermocouple (iron-constantan) placed into the thermowell extending horizontally in the reactor.

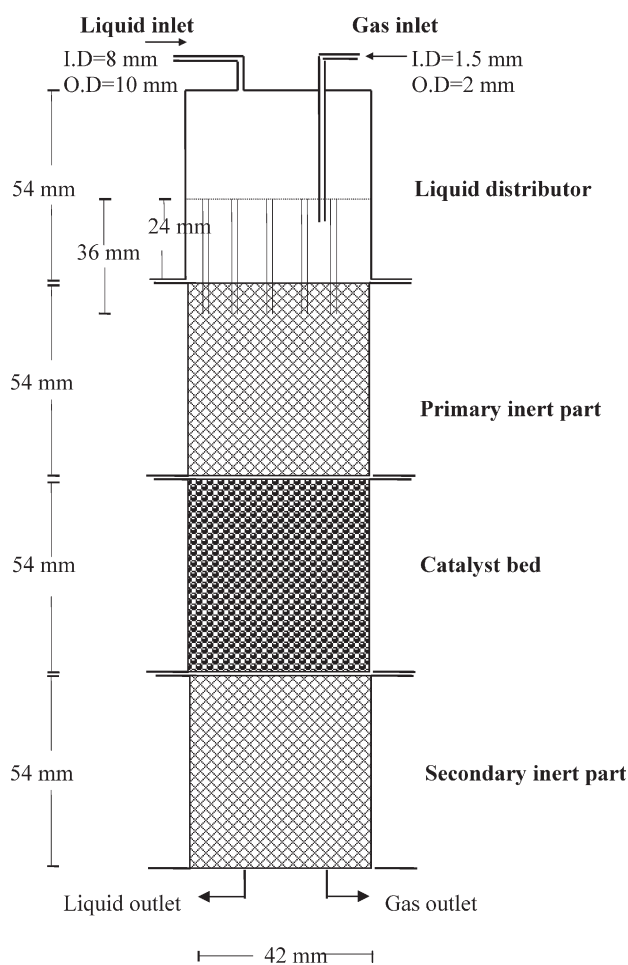


Fig. 2 – Trickle-bed reactor

## Analysis

The expected reaction products are butanol and butyraldehyde. In the experiments on the Pd based commercial catalyst only butyraldehyde and crotonaldehyde peaks were identified in the reaction products.

The stream leaving the reactor is passed through the coil type cooler in which the coolant (ethylalcohol-water mixture) is circulated. The cooled stream is collected in a container and the leaving gas is purged to the atmosphere. The container is discharged at the end of each experiment (reaction generally lasts 3 h) and the samples are taken for analysis. The analyses of the samples are repeated for two or three times. A Hewlett Packard 5890 Series II Gas Chromatograph with flame ionization detector and HP integrator are used to make analysis of the liquid products. A polar capillary column (HP-FFAP, 25 m · 0.32 mm · 0.52 μm) is used, nitrogen is the carrier gas for the analyses. The temperatures of injection and detector are 160 and 250 °C, respectively.

## Procedures

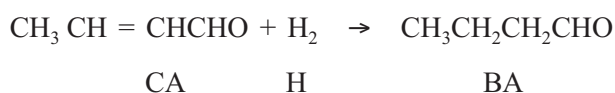
After the fresh catalyst is loaded and activated, reactor and preheater are heated to required temperatures. The cooling fluid (alcohol-water) is circulated through the cooler. Crotonaldehyde is charged to graduated cylinder. The pump is activated and its speed is adjusted to obtain the desired flow rate of crotonaldehyde. The time and the liquid level in the measuring cylinder are recorded. Then hydrogen flow rate is adjusted by the valve on the calibrated rotameter and sent to the reactor. It is waited until the system reaches steady state. It means that, the flow rates of crotonaldehyde and hydrogen, the temperatures of reactor and preheater are remained constant at adjusted values. At the end of 3 h the run is ended, hydrogen gas and the pump are switched off. The level in the feed cylinder is recorded and the cooling fluid circulation is stopped.

The reaction products collected in the container is discharged by the valve and the sample is taken for analysis. At the end of each experiment, nitrogen gas is passed through the reactor at very low flow rate (36 ml min<sup>-1</sup>) to clean the catalyst any impurities as recommended in the literature.<sup>20</sup>

## Results and discussion

The experiments are collected in the two categories as preliminary and kinetic experiments. In both experiment groups, the experiments are carried out at atmospheric pressure by changing temperature and flow rates of crotonaldehyde and hydrogen.

In the preliminary experiments, firstly the liquid phase hydrogenation catalysts supplied from different catalyst manufacturers were tested and the appropriate catalyst converting crotonaldehyde to butyraldehyde was chosen, then the ranges of the flow rates of crotonaldehyde and hydrogen, which maintain trickle-flow conditions, were searched for and then the experiments were performed to determine the appropriate temperature range. The experiments were evaluated by calculating conversion values by the help of the results of gas chromatograph analyses and by the following reaction scheme:



So, the weight percent of butyraldehyde is,

$$w_{\text{BA}} = \frac{(F_{\text{CA}0} \cdot x_{\text{CA}}) \cdot 72}{70[F_{\text{CA}0}(1 - x_{\text{CA}})] + (F_{\text{CA}0} \cdot x_{\text{CA}}) \cdot 72} \quad (1)$$

and finally the conversion of crotonaldehyde to the butyraldehyde is:

$$x_{CA} = \frac{35 \cdot (\text{wt}\%CA)}{36 - (\text{wt}\%CA)} \cdot 100 \quad (2)$$

Conversions were plotted versus the searched operating condition values, while the another conditions were kept constant, and the optimum range of the searched operating condition was determined by evaluating the preliminary experiments.

#### Determination of trickle flow conditions

The ranges of the flow rates of crotonaldehyde and hydrogen which maintain trickle-flow conditions were decided by calculating the Reynolds numbers. The flow rates to be used were limited by the operating range of the pump used to transport crotonaldehyde to the reactor and by the operating range of the rotameter that was used to adjust the flow rate of hydrogen. Depending on the literature information the ranges of the flow rates in which Reynolds numbers satisfy the trickle flow condition were found up to  $1.9 \text{ ml min}^{-1}$  for crotonaldehyde and up to  $1000 \text{ ml min}^{-1}$  for hydrogen.<sup>21</sup>

#### Effect of hydrogen and crotonaldehyde flow rates

An experiment-set was performed at  $60^\circ\text{C}$  and at constant crotonaldehyde flow rate of  $0.45 \text{ ml min}^{-1}$  (it has satisfied the trickle flow condition) to decide the range of the hydrogen flow rate (Fig. 3). It is seen from Figure 3 that, the flow rate values greater than  $400 \text{ ml min}^{-1}$  can be recommended as confidential to be able to neglect mass transfer limitations. It is relevant to operate the reactor at  $400 \text{ ml min}^{-1}$  hydrogen flow rate as a hydrogen consumption point of view and the satisfaction of the trickle flow conditions.

The another experiment-set was performed at  $45^\circ\text{C}$  and at constant hydrogen/crotonaldehyde mol ratio of 2:1 to decide the value of LHSV (Fig. 4).

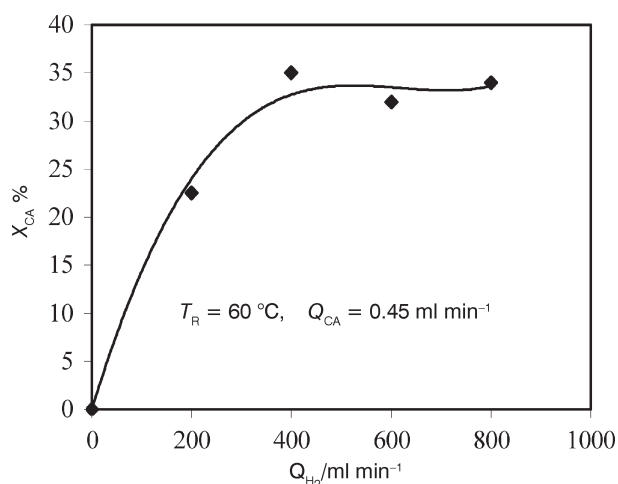


Fig. 3 – Conversion vs hydrogen flow rate

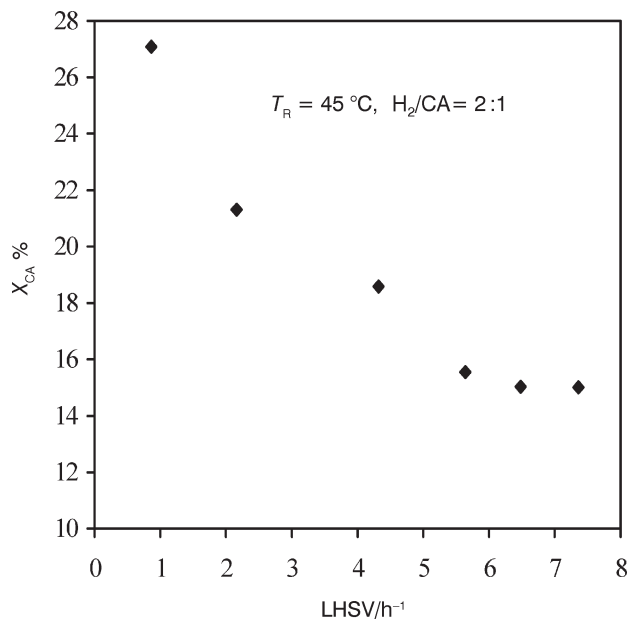


Fig. 4 – Conversion vs LHSV

The hydrogen/crotonaldehyde mol ratio of 2:1 is recommended for the catalyst supplied from Süd Chemie AG. It can be easily seen from Figure 4 that crotonaldehyde conversion to butyraldehyde decreases as LHSV increases as expected. The range of the feed flow rate of crotonaldehyde was chosen as  $0.4 - 1.9 \text{ ml min}^{-1}$  in this study. The value of LHSV with respect to the lowest feed flow rate of crotonaldehyde ( $0.4 \text{ ml min}^{-1}$ ) was around  $2 \text{ h}^{-1}$  and this value satisfies the trickle flow condition. So it was decided from Figure 4 that, the value of LHSV should be above  $2 \text{ h}^{-1}$  to maintain differential reactor conditions.

#### Effect of reaction temperature

To decide the appropriate reaction temperature range, the five experiments were carried out at  $30 - 50^\circ\text{C}$ , at constant hydrogen/crotonaldehyde ratio and constant value of LHSV. Figure 5 represents conversion values versus temperature at constant hydrogen/crotonaldehyde ratio. As it can be seen from Figure 5 that the conversion increases sharply as the temperature exceeds  $45^\circ\text{C}$ . To maintain the controlled progression of the reaction, the temperature should not be higher than  $50^\circ\text{C}$ .

#### Kinetics study

The experiments were performed at the decided experimental conditions. The operating conditions of kinetic experiments are given in Table 1. It can be easily seen from Table 1 that the smallest conversion was 5.28 % and the highest conversion was 39.63 %. The data between space time ( $m_w/F_{CA0}$ ) and conversion ( $X_{CA}$ ) were plotted (Figure 6) at dif-



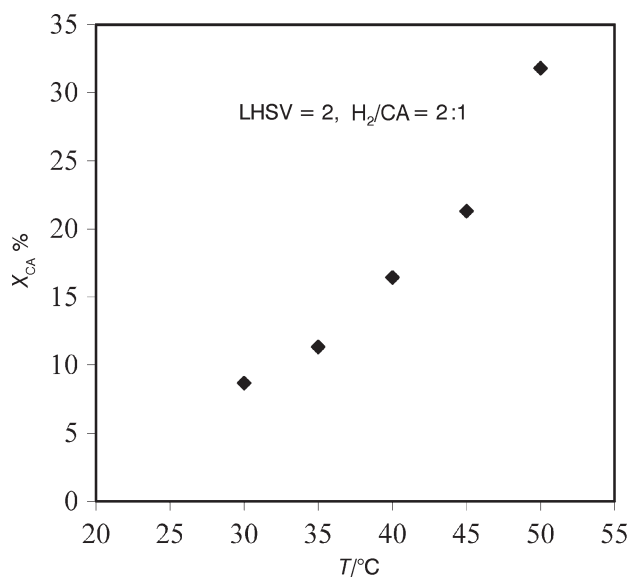
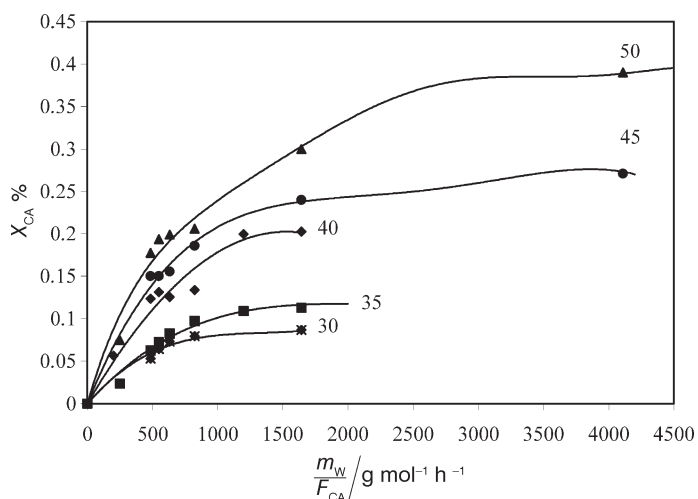


Fig. 5 – Conversion vs temperature

Fig. 6 – Conversion vs  $m_w/F_{CA0}$ 

ferent temperatures and the relationships between these two parameters were explained by the equation given below:

$$X_{CA} = \frac{a \cdot (m_w/F_{CA0})}{b + (m_w/F_{CA0})} \quad (3)$$

The constants  $a$  and  $b$  determined at each temperature are collected in Table 2. The accordance of derived relations with the experimental points can be seen in Figure 6. It can be seen from Figure 6 that, conversion increases with increasing temperature as expected. The reaction rates at different temperatures are calculated by differentiating the derived relations. They are given in Table 3. As it can be seen from the table, that the experiments could not be performed at some particular space-time ( $m_w/F_{CA0}$ ) values due to the limitations in the appa-

Table 1 – The operating conditions of the kinetic experiments

$T_R / ^\circ\text{C}$	$Q_{CA} / \text{ml min}^{-1}$	$Q_{H_2} / \text{ml min}^{-1}$	$X_{AC} / \%$
30	0.50	300	8.68
30	1.00	595	7.96
30	1.30	729	7.32
30	1.50	892	6.43
30	1.70	1040	5.28
35	0.50	300	8.12
35	0.66	393	10.95
35	1.00	595	8.43
35	1.30	729	8.27
35	1.50	892	7.28
35	1.70	1040	6.28
40	0.50	300	20.26
40	1.00	595	13.39
40	1.30	729	12.55
40	1.50	892	8.62
40	1.70	1040	12.37
40	1.50	892	10.18
45	0.20	120	27.09
45	0.50	300	21.31
45	1.10	654	18.59
45	1.30	729	15.56
45	1.50	892	15.03
45	1.70	1040	15.01
50	0.20	120	39.63
50	0.50	300	31.79
50	0.80	535	26.03
50	1.00	595	20.61
50	1.30	729	19.93
50	1.50	892	19.36
50	1.70	1040	17.74

Table 2 – The constants,  $a$  and  $b$ , at different temperatures

$T, ^\circ\text{C}$	$a$	$b$
30	0.1043	330.821
35	0.1814	913.041
40	0.3347	984.879
45	0.2954	484.620
50	0.4673	774.308

Table 3 – Reaction rates and conversions

$m_w/F_{CA0}$ g min mol <sup>-1</sup>		$T = 30\text{ }^\circ\text{C}$	$T = 35\text{ }^\circ\text{C}$	$T = 40\text{ }^\circ\text{C}$	$T = 45\text{ }^\circ\text{C}$	$T = 50\text{ }^\circ\text{C}$
4108.4	$(-r_{CA}) \cdot 10^5$	*	*	*	0.68	1.52
	$X_{CA}$				0.271	0.396
1643.4	$(-r_{CA}) \cdot 10^5$	0.88	2.53	4.77	3.16	6.19
	$X_{CA}$	0.087	0.113	0.221	0.240	0.260
1200	$(-r_{CA}) \cdot 10^5$	*	3.71	6.91	*	*
	$X_{CA}$		0.109	0.199		
1027.1	$(-r_{CA}) \cdot 10^5$	*	*	*	*	11.14
	$X_{CA}$					
821.7	$(-r_{CA}) \cdot 10^5$	2.60	5.50	10.10	8.39	14.19
	$X_{CA}$	0.079	0.098	0.134	0.186	0.206
632.1	$(-r_{CA}) \cdot 10^5$	3.72	6.94	12.61	11.48	18.28
	$X_{CA}$	0.073	0.083	0.125	0.155	0.199
547.8	$(-r_{CA}) \cdot 10^5$	4.47	7.76	14.03	13.43	20.69
	$X_{CA}$	0.064	0.073	0.132	0.150	0.194
483.3	$(-r_{CA}) \cdot 10^5$	5.21	8.49	15.29	15.28	22.86
	$X_{CA}$	0.053	0.063	0.124	0.150	0.177
250	$(-r_{CA}) \cdot 10^5$	*	12.24	23.48	*	*
	$X_{CA}$		0.024	0.056		

\*No experiment was carried out at this value.  $r_{CA}$  /mol g<sub>cat</sub><sup>-1</sup> min<sup>-1</sup>

ratus. When the space-time values increase or crotonaldehyde flow rate decreases, the reaction rate increases with increasing temperature. It is also seen from Table 3 that, the experimental reaction rates are very high if they are compared with other hydrogenation reactions in the literature. The higher rate is interpreted as a nature of a system in which pores of catalyst were filled with liquid vapour and hydrogen and diffusion limitations are negligible. Sedriks and Kenney reported this effect in the study of the hydrogenation of crotonaldehyde.<sup>4,22</sup>

To elaborate the kinetic expression of the reaction, first five different models given in Appendix were derived according to LHHW mechanism in the light of literature information.<sup>21</sup> The parameters seen in the models were determined by linearizing the equations and using linear regression technique. One of the main criteria to test the models was to obtain positive values for all of the parameters. Only the second model at the two temperatures studied, of 303 and 308 K, satisfied this criterion. It was seen that the rate constant decreased with increasing temperature. So it was decided that these proposed models were not suitable for the experimental data obtained from this study.

Second, the kinetics of the reaction was determined by formulating a rate of equation with pre-supposed exponents on the concentration terms and by fitting experimental data to the rate equation.

As it is known the one of the important design parameters in a trickle bed reactor is wetting of catalyst. At low liquid and gas velocities, the gas phase is continuous and the liquid falls in rivulets from one particle to the next (trickle-flow regime). Hence for a bed where any part of the catalyst remains dry, the contribution to the overall rate of the **wet** and **dry** catalyst must be considered separately.<sup>4</sup>

#### a) Wet catalyst:

For wet catalyst, the reaction occurs between the crotonaldehyde on the catalyst surface and the hydrogen, both coming by two ways:

- 1) from liquid to solid and
- 2) from gas to solid.

Considering the reaction to be irreversible, the reaction rate can be expressed for wet catalyst bed as follows:

$$r_T = f k_1 (\bar{c}_{H_2})_s^m (\bar{c}_{CA})_s^n + (1-f) k_2 (\bar{c}_{H_2})_g^{m'} (\bar{c}_{CA})_s^{n'} \quad (4)$$

(liquid phase reaction)      (gas phase reaction)

where;

$k_1$  and  $k_2$  : Reaction rate constants,

$(\bar{c}_{H_2})_s$ : Mean concentration of hydrogen transported from liquid phase to catalyst surface (mol  $\text{cm}^{-3}$ ),

$$(\bar{c}_{H_2})_s = \frac{(c_{H_2s}) - (c_{H_2})_{ls}}{\ln \frac{(c_{H_2s})}{(c_{H_2})_{ls}}} \quad (5)$$

$(c_{H_2})_s$ : concentration of hydrogen on liquid-solid interphase at the inlet of the reactor (mol  $\text{cm}^{-3}$ ),

$(c_{H_2})_{ls}$ : concentration of hydrogen on liquid-solid interphase at the exit of the reactor (mol  $\text{cm}^{-3}$ ),

$(\bar{c}_{H_2})_g$  : mean concentration of hydrogen transported from gas phase to catalyst surface (mol  $\text{cm}^{-3}$ ),

$$(\bar{c}_{H_2})_g = \frac{(c_{H_2})_{gs} - (c_{H_2})_s}{\ln \frac{(c_{H_2})_{gs}}{(c_{H_2})_s}} \quad (6)$$

$(c_{H_2})_{gs}$ : concentration of hydrogen on gas-solid interphase at the inlet of the reactor (mol  $\text{cm}^{-3}$ ),

$(c_{H_2})_s$ : concentration of hydrogen on gas-solid interphase at the exit of the reactor (mol  $\text{cm}^{-3}$ ),

$(\bar{c}_{CA})_s$ : mean concentration of crotonaldehyde on solid surface interface (mol  $\text{cm}^{-3}$ ),

$$(\bar{c}_{CA})_s = \frac{(c_{CA_s}) - (c_{CA})}{\ln \frac{(c_{CA_s})}{(c_{CA})}} \quad (7)$$

$(c_{CA_s})$ : concentration of crotonaldehyde on liquid-solid interphase at the inlet of the reactor (mol  $\text{cm}^{-3}$ ),

$(c_{CA})$ : concentration of crotonaldehyde on liquid-solid interphase at the exit of the reactor (mol  $\text{cm}^{-3}$ ),

$f$ : fraction of active catalyst surface wetted,

$m, n, m', n'$ : orders of the reaction with respect to the reactants for liquid to solid and gas to solid, respectively.

To calculate the surface concentrations for crotonaldehyde and hydrogen, first liquid phase mass transfer coefficient ( $k_L$ ) of hydrogen was calculated using Simple Stagnant Film Theory.<sup>8</sup>

$$k_L = \frac{2D a}{H_0} \quad (8)$$

$H_0$  is the external holdup in the bed and given by the correlation:<sup>23</sup>

$$H_0 = A u_1^{1/3} \mu_1^{1/4} + B \quad (9)$$

Liquid-solid mass transfer coefficient ( $k_s$ ) was calculated for hydrogen using equation 10:

$$k_s = k_L = \frac{2D a}{H_0} \quad (10)$$

Liquid-solid mass transfer coefficient ( $k_s a$ ) was calculated for crotonaldehyde using the following correlation:<sup>24</sup>

$$(k_s a)_{CA} = 1596 \frac{D_{CA}}{\rho_P d_P^2} Re_L^{1.15} Sc_L^{0.33} \quad (11)$$

Gas-solid mass transfer coefficient ( $k_{gs} a$ ) was also calculated using the following correlation:<sup>25</sup>

$$\frac{k_{gs} a}{D} = 63 \cdot 10^4 * H_d^{2.5} * Sc_L^{0.5} \quad (12)$$

Mass transfer coefficients were calculated as described above. Surface concentrations for crotonaldehyde and hydrogen were obtained and the mean concentrations were given in Table 4.

## b) Dry catalyst:

It was suspected that any part of the catalyst remains dry, so the reaction could be occurred between hydrogen and crotonaldehyde coming directly from gas phase to catalyst surface. The reaction rate can be expressed for a dry catalyst bed as follows:

$$r_T = k_1 (\bar{c}_{H_2})_g^{m'} (\bar{c}_{CA})_s^{n'} \quad (13)$$

The reaction rate equations were solved by the linear (for dry catalyst) and nonlinear (for wet catalyst) regression programs that minimize the summation of squares of the errors between experimental reaction rates and calculated reaction rates by the model.

When the concentration values in the Table 4 are investigated, it can be seen that surface concentration of hydrogen can not be calculated at some experiments, which were carried out at high temperatures and high crotonaldehyde flow rates. Depending on this finding the experiments performed at 30, 35 °C were evaluated according to wet catalyst assumption and another set performed at 40, 45, 50 °C, was evaluated for dry catalyst.

The change of reaction rate coefficient,  $k_1$  and  $k_2$  with varying temperature are given in Table 5.

The reaction rate expression was rearranged by adding fraction ( $f$ ) term into reaction rate coefficients ( $k_1, k_2$ ) to create a common expression as the function of the temperature. According to the calculated values the computed reaction rate expressions can be written as follows:

Table 4 – Mean concentrations of crotonaldehyde and hydrogen

$T/^\circ\text{C}$	$(\bar{c}_{\text{H}_2})_g \cdot 10^5$ mol cm <sup>-3</sup>	$(\bar{c}_{\text{H}_2})_s \cdot 10^6$ mol cm <sup>-3</sup>	$(\bar{c}_{\text{CA}})_s$ mol cm <sup>-3</sup>
30	3.860	3.345	0.01162
	3.857	2.626	0.01167
	3.859	2.081	0.01172
	3.865	1.692	0.01177
	3.874	1.322	0.01182
35	3.752	2.710	0.01145
	3.751	2.022	0.01148
	3.762	1.190	0.01155
	3.774	4.844	0.01165
	3.783	5.754	0.01171
	3.792	–	0.01177
40	3.574	1.465	0.01086
	3.571	0.592	0.01088
	3.633	–	0.01132
	3.641	–	0.01137
	3.633	–	0.01133
	3.639	–	0.01138
45	3.500	2.755	0.01042
	3.532	1.976	0.01080
	3.540	–	0.01099
	3.562	–	0.01118
	3.562	–	0.01121
	3.558	–	0.01121
50	3.300	2.261	0.00954
	3.335	0.641	0.01114
	3.365	–	0.01048
	3.423	–	0.01084
	3.425	–	0.01088
	3.426	–	0.01092
3.437	–	0.01103	

For wet catalyst:

$$r_{\text{Tot}} = (86.87 - 0.256T) \cdot 10^{18} e^{-\frac{122352}{RT}} * c_{\text{H}_2\text{s}}^{0.5} * c_{\text{CA}_s}^{0.854} + (0.0662T - 19.254) e^{-\frac{8623.28}{RT}} * c_{\text{H}_2\text{gs}}^{0.47} * c_{\text{CA}_s}^{0.4} \quad (15)$$

For dry catalyst:

$$r_{\text{Tot}} = 3.076 \cdot 10^6 e^{-\frac{45184.14}{RT}} * c_{\text{H}_2\text{gs}}^{0.455} * c_{\text{CA}_s}^{0.445} \quad (16)$$

Comparison of the experimental and calculated reaction rates is seen from Figure 7.

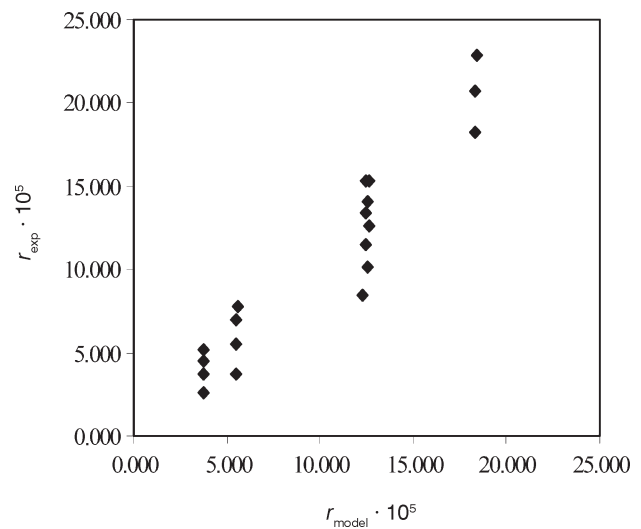


Fig. 7 – Comparison of the experimental and calculated reaction rates

The effect of internal mass transfer on reaction kinetics was searched for, both, experimentally and theoretically. The experiments were carried out to evaluate the effect of pore diffusion in the catalyst by recording conversions on three different diameter of catalyst particles ( $d_p = 3, 4,$  and above  $4$  mm) at  $50^\circ\text{C}$  and at a value of LHSV of  $2.22 \text{ h}^{-1}$  (Figure 8).

Table 5 – Reaction rate constants,  $k_1$  and  $k_2$ 

$T / ^\circ\text{C}$	$k_1$	$k_2$	$m$	$n$	$m'$	$n'$	$f$
	$\frac{\text{mol}^{1-m'-n'}}{\text{ml}^{m'+n'} \text{g}_{\text{cat}}^{-1} \text{min}^{-1}}$	$\frac{\text{mol}^{1-m-n}}{\text{ml}^{m+n} \text{g}_{\text{cat}}^{-1} \text{min}^{-1}}$					
30	$1.05 \cdot 10^{-1}$	$1.0 \cdot 10^{-2}$	0.5	0.854	0.470	0.400	0.752
35	$1.11 \cdot 10^{-1}$	$2.2 \cdot 10^{-2}$	0.5	0.854	0.470	0.400	0.647
40	–	$9.67 \cdot 10^{-2}$	–	–	0.455	0.445	–
45	–	$9.73 \cdot 10^{-2}$	–	–	0.455	0.445	–
50	–	$1.66 \cdot 10^{-1}$	–	–	0.455	0.445	–



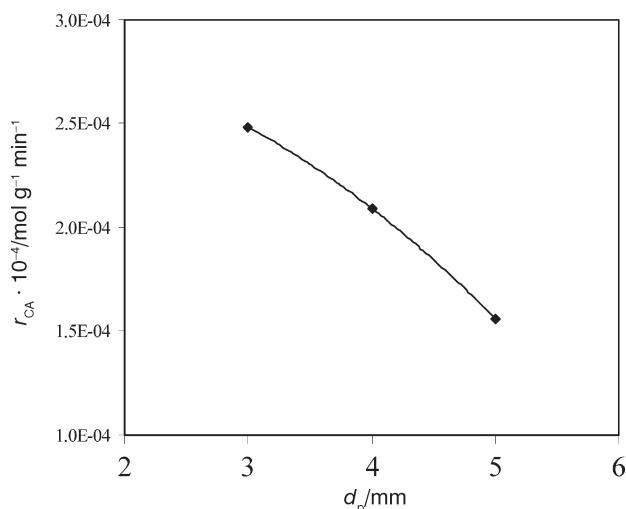


Fig. 8 – Effect of particle size on rate of reaction

From the literature approach<sup>6</sup> it is expected that as the particle diameter is increased, the rate would not be affected if internal resistances could be neglected. It is seen from Figure 8, when the particle diameter is increased, the rate decreases. So the internal effect could not be neglected. This finding was also proved with the theoretical calculation of the effectiveness factor according to the procedure given in the literature.<sup>26,27</sup>

$$\phi = \frac{d_p}{6} r(c_s) \rho_{\text{Bed}} \left[ 2 \int_0^{c_s} D_e r \rho_{\text{Bed}} dc \right]^{-0.5} \quad (17)$$

$$\eta = \frac{1}{\phi} \left[ \frac{1}{\tanh 3\phi} - \frac{1}{3\phi} \right] \text{ for spherical particles} \quad (18)$$

where;

$\phi$ : Thiele modulus

$\rho_B$ : bulk density of catalyst, 0.65 g cm<sup>-3</sup>

$D_e$ : effective diffusion coefficient (cm<sup>2</sup> s<sup>-1</sup>)

$\eta$ : effectiveness factor.

It was seen from Table 6, that the values of Thiele modulus were above 5 for wet catalyst (at  $T = 30$  and  $35$  °C) and they were around 1 for dry catalyst (at  $T = 40$  to  $50$  °C).

If Thiele modulus  $> 5$ ,  $\eta \cong 1/\phi$ . Practically, these conditions mean that diffusion into the pellet is relatively slow, so that the reaction occurs before the reactant has diffused into the pellet<sup>27</sup>. When the Thiele modulus is large, diffusion usually limits the overall rate of reaction<sup>24</sup>.

The rate equation derived previously only took external mass transfer effects into the consideration. Intrinsic rates should be determined by dividing the derived reaction rates by the effectiveness factors.

In the literature, many researchers have studied the kinetics of hydrogenation reactions. Generally reaction rate is expressed by the following equation:

$$-r_p = k \cdot c_{\text{CA}}^m \cdot c_{\text{H}_2}^n \quad (19)$$

As an example, in the study on the hydrogenation of methylacetylene with a supported group VIII metals the reaction rate could be described by equation 19; the reaction orders were highly dependent on the experimental conditions.<sup>28</sup>

The kinetic evaluation showed that the apparent activation energies are between 125.60 – 276.32 kJ mol<sup>-1</sup> (30.0 – 66.0 kcal mol<sup>-1</sup>) in trickle bed reactor. In the literature the apparent activation energy was given as 46.05 kJ mol<sup>-1</sup> (11 kcal mol<sup>-1</sup>) for the hydrogenation of crotonaldehyde by using slurry reactor.<sup>22</sup> Also it was mentioned that the activation energy on the same type of catalyst changed from 68.53 to 88.59 kJ mol<sup>-1</sup> (16.37 to 21.16 kcal mol<sup>-1</sup>) in the studies employed by several workers<sup>29</sup>. On palladium alumina catalyst, activation energy was around 54.30 kJ mol<sup>-1</sup> (12.97 kcal mol<sup>-1</sup>). In short, the activation energies depend on the process and the catalyst characterization.

Table 6 – Calculated Thiele moduli and effectiveness factors

$\frac{T}{^\circ\text{C}}$	$\phi$				$\eta$			
	LHSV				LHSV			
	3.9 h <sup>-1</sup>	5.07 h <sup>-1</sup>	5.85 h <sup>-1</sup>	6.63 h <sup>-1</sup>	3.9 h <sup>-1</sup>	5.07 h <sup>-1</sup>	5.85 h <sup>-1</sup>	6.63 h <sup>-1</sup>
30	5.07	6.16	7.37	9.18	0.475	0.408	0.352	0.291
35	8.75	14.23	33.68	277.2	0.303	0.196	0.086	0.011
40	1.249	1.249	1.249	1.250	0.909	0.9092	0.9092	0.9092
45	1.454	1.458	1.459	1.459	0.882	0.881	0.881	0.881
50	1.704	1.705	1.707	1.709	0.848	0.847	0.847	0.847

\*: Temperatures of 30, 35 °C represent wet condition and 40, 45, 50 °C represent dry condition.

## Conclusions

According to the obtained results the following conclusions can be stated:

1. The ranges of the flow rates of crotonaldehyde and hydrogen which maintain trickle flow conditions were decided by calculating the Reynolds numbers. Reynolds numbers satisfying the trickle flow condition were found corresponding up to 0.9 ml min<sup>-1</sup> for crotonaldehyde and up to 1000 ml min<sup>-1</sup> for hydrogen.

2. It is possible to state temperature range between 30 – 50 °C to investigate the reaction kinetics.

3. The kinetic parameters from the conversion-space time data can be estimated.

4. The wetting of the catalyst was found to be important parameter and it was seen from the results that the wetting is incomplete and reaction on the dry catalyst may be come dominant on the overall reaction rate at high temperatures. The wetting was expressed as a function of the temperature.

5. It was found that the external mass transfer effects played an important role on the reaction kinetics. Especially the mass transfer of hydrogen from bulk gas to gas-liquid interphase was very effective.

6. The internal resistances have been also researched and it has been proved experimentally and theoretically that the intra-particle diffusion effects could not be neglected.

7. For wet catalyst reaction it was found to be 0.854 with respect to crotonaldehyde and 0.5 with respect to hydrogen for liquid phase; reaction was found to be 0.4 with respect to crotonaldehyde and 0.47 with respect to hydrogen for gas phase.

8. For dry catalyst reaction was found to be of 0.455 with respect to crotonaldehyde and 0.445 with respect to hydrogen.

9. The activation energies were found to be between 125.60 – 276.32 kJ mol<sup>-1</sup> (30.0 – 66.0 kcal mol<sup>-1</sup>). It is apparent that the activation energies found in this study are higher than in another hydrogenation reactions. This can be explained that energy barrier, which is overcome for the accomplishment of the reaction is higher than in slurry reactor.

## APPENDIX

### Models

$$a = 0.5, 1; b = 1$$

$$1. \quad -r_{CA,s} = \frac{k c_{H_2,s}^a c_{CA,s}^b}{(1 + K_{H_2} c_{H_2,s} + K_{CA} c_{CA,s})^2}$$

$$2. \quad -r_{CA,s} = \frac{k c_{H_2,s}^a c_{CA,s}^b}{(1 + K_{H_2} c_{H_2,s})^4}$$

$$3. \quad -r_{CA,s} = \frac{k c_{H_2,s}^a c_{CA,s}^b}{(1 + \sqrt{K_{H_2} c_{H_2,s}} + K_{CA} c_{CA,s})^3}$$

$$4. \quad -r_{CA,s} = \frac{k c_{H_2,s}^a c_{CA,s}^b}{(1 + \sqrt{K_{H_2} c_{H_2,s}})^2}$$

$$5. \quad -r_{CA,s} = \frac{k c_{H_2,s}^a c_{CA,s}^b}{1 + K_{CA} c_{CA,s}}$$

### Nomenclature

$A, B$  – constants characteristics of the particle diameter and shape (0.102 and 0.01, respectively).

$c$  – concentration, mol cm<sup>-3</sup>

$d$  – diameter, mm

$D$  – molecular diffusivity of hydrogen, cm<sup>2</sup> sec<sup>-1</sup>

$D_R$  – reactor diameter

$\eta$  – effectiveness factor

$f$  – fraction of active catalyst surface wetted

$\varphi$  – Thiele modulus

$F_{A0}$  – molar flow rate of reactant, mol h<sup>-1</sup>

$H_d$  – dynamic holdup

$H_0$  – external holdup

$H_2/CA$  – molar ratio

$k_1, k_2$  – reaction rate constants

$k_L$  – mass transfer coefficient from gas-liquid interface into liquid bulk, cm sec<sup>-1</sup>

$k_S$  – mass transfer coefficient of hydrogen from liquid bulk to solid, cm sec<sup>-1</sup>

LHSV – liquid hourly space velocity, h<sup>-1</sup>

$\mu$  – viscosity, mPa s

$Q$  – volumetric flow rate, cm<sup>3</sup> min<sup>-1</sup>

$r$  – global reaction rate, mol g<sup>-1</sup> h<sup>-1</sup>

$Re$  – Reynolds number

$Sc$  – Schmidt number

$s$  – specific surface area, m<sup>2</sup> g<sup>-1</sup>

$T$  – temperature, °C, K

$u$  – superficial velocity, cm sec<sup>-1</sup>

$m_w$  – catalyst mass, g

$X$  – conversion, 1

$\rho$  – density

$w$  – weight percent

$\tau$  – space time

$\sigma$  – standard error

### Abbreviations and subscriptions

BA	– butyraldehyde
CA	– crotonaldehyde
exp	– experimental
g	– gas
H <sub>2</sub>	– hydrogen
i	– interface
l, L	– liquid
<i>m, n, m', n'</i>	– exponents
Mix.	– mixture
p	– catalyst pellet
St.St.	– steady state
Tot	– Total

### Literature

1. *Mc Ketta, J. J., Cunnigham, W. A.*, Encyclopedia of Chemical Processing and Design. 1, Marcel Dekker, Inc., New York, 1976.
2. *Hahn, H. D., Dambkes, G., Rupprich, N.*, Butanols. Ulmann's Ency. Of Industrial Chemistry, A4, 463-472, 1985.
3. Kirk-Othmer Encyclopedia of Chemical Technology. Butyraldehyde. Kirk-Othmer Encyclopedia of Chemical Technology, 4, 338, 1978.
4. *Sedriks, W., Kenney, C. N.*, Chem. Eng. Sci., **28** (1973) 559.
5. *Herskowitz, M., Carbonel, R. G., Smith, J. M.*, AIChE J. **25** (1979) 272.
6. *Sharma, S. D., Gadgil, K., Sarkar, M. K.*, Chem. Eng. Technol. **16** (1993) 347.
7. *Zhu, D. X., Hofmann, H.*, Chem. Eng. Technol. **20** (1997) 131.
8. *Satterfield, C. N.*, AIChE J. **21** (1975) 209.
9. *Herskowitz, M., Smith, J. M.*, AIChE J. **29** (1983) 1.
10. *Leung, P. C., Smith, J. M.*, AIChE J. **33** (1987) 996.
11. *Vannice, A. M., Sen, B.*, J. of Catal. **115** (1989) 65.
12. *English, M., Jentys, A., Lercher, J. A.*, J. of Catal. **166** (1997) 25.
13. *Pai, C. C.*, Canadian Patent, (1980) 1137519.
14. *Gutierrez-Ortiz, M. A., Gonzalez-Marcos, J. A., Gonzalez-Marcos, P. M., Gonzalez-Velasco, J. R.*, Ind. Eng. Chem. Res. **32** (1993) 1035.
15. *Makoungou, R. M., Murzin, D. Y., Dauscher, A. E., Touroude, R. A.* Ind. Eng. Chem. Res. **33** (1994) 1881.
16. *Consonni, M., Touroude, R., Murzin, D. Y.*, Chem. Eng. Technol. **21** (1998) 605.
17. *Salman, F., Park, C., Baker, R. T. K.*, Catalysis Today **53** (1999) 385.
18. *Uygur, H., Atalay, S., Savaşç2, T. Ö.*, J. of Chem. Eng. Japan **31** (1998) 178.
19. *Attou, A., Boyer, C., Ferschneider, G.*, Chem. Eng. Sci. **54** (1999) 785.
20. *Logsdon, J. E., Loke, R. A., Merriam, J. S., Voight, R. W.*, European Patent, 0269888, 1987.
21. *Froment, G. F., Bischoff, K. B.*, Chemical Reactor Analysis and Design; 711, John Wiley&Sons, New York, 1979.
22. *Kenney, C. N., Sedriks, W.*, Chem. Eng. Sci. **27** (1972) 2029.
23. *Satterfield, C. N., Way, P. F.*, AIChE J. **18** (1972) 305.
24. *Fogler, H. S.* Elements of Chemical Reaction Engineering, 597, Prentice-Hall Inc., USA, 1986.
25. *Turek, F., Lange, R.*, Chem. Eng. Sci. **36** (1981) 569.
26. *Goto, S., Smith, J. M.*, AIChE J. **21** (1975) 714.
27. *Smith, J. M.*, Chemical Engineering Kinetics; McGraw-Hill Int. Ed., 1981. pp 434-435,
28. *Kiperman, S. L.*, Some Problems of Chemical Kinetics in Heterogeneous Hydrogenation Catalysis. Catalytic Hydrogenation edited by Cerveny L., Chp.1, pp 1-52, Elsevier Science, Netherlands, 1986.
29. *Wehrli, J. T., Thomas D. J., Wainwright M. S., Trimm D. L., Cant N.*, Catalytic Science and Technology **1** (1991a).